

# Star Formation in the Multiverse

---

**Raphael Bousso and Stefan Leichenauer**

*Center for Theoretical Physics, Department of Physics  
University of California, Berkeley, CA 94720-7300, U.S.A.*

and

*Lawrence Berkeley National Laboratory, Berkeley, CA 94720-8162, U.S.A.*

**ABSTRACT:** We develop a simple semi-analytic model of the star formation rate (SFR) as a function of time. We estimate the SFR for a wide range of values of the cosmological constant, spatial curvature, and primordial density contrast. Our model can predict such parameters in the multiverse, if the underlying theory landscape and the cosmological measure are known.

---

## Contents

<b>1. Introduction</b>	<b>1</b>
<b>2. Model</b>	<b>2</b>
2.1 Goals	2
2.2 Geometry and initial conditions	4
2.3 Linear perturbation growth and halo formation	5
2.4 Cooling and galaxy formation	8
2.5 Star formation	10
<b>3. Results</b>	<b>13</b>
3.1 Our universe	13
3.2 Varying single parameters	15
3.3 Varying multiple parameters	20

---

## 1. Introduction

In this paper, we study cosmological models that differ from our own in the value of one or more of the following parameters: The cosmological constant, the spatial curvature, and the strength of primordial density perturbations. We will ask how these parameters affect the rate of star formation (SFR), i.e., the stellar mass produced per unit time, as a function of cosmological time.

There are two reasons why one might model the SFR. One, which is not our purpose here, might be to *fit* cosmological or astrophysical parameters, adjusting them until the model matches the observed SFR. Our goal is different: We would like to *explain* the observed values of parameters, at least at an order-of-magnitude level. For this purpose, we ask what the SFR would look like if some cosmological parameters took different values, by amounts far larger than their observational uncertainty.

This question is reasonable if the observed universe is only a small part of a multi-universe, in which such parameters can vary. This situation arises when there are multiple long-lived vacua, such as in the landscape of string theory. It has the potential to explain the smallness of the observed cosmological constant [1], as well as other unnatural

coincidences in the Standard Model and in Standard Cosmology. Moreover, a model of star formation can be used to test the landscape, by allowing us to estimate the number of observers that will observe particular values of parameters. If only a very small fraction of observers measure the values we have observed, the theory is ruled out.

The SFR can be related to observers in a number of ways. It can serve as a starting point for computing the rate of entropy production in the universe, a well-defined quantity that appears to correlate well with the formation of complex structures such as observers [2]. (In our own universe, most entropy is produced by dust heated by starlight [3].) Alternatively, one can posit that a fixed (presumably very small) average number of observers arises per star, perhaps after a suitable delay time of order billions of years.

To predict a probability distribution for some parameter, this anthropic weighting must be combined with the statistical distribution of parameters in the multiverse. Computing this distribution requires at least statistical knowledge of the theory landscape, as well as understanding the measure that regulates the infinities arising in the eternally inflating multiverse. Here, we consider none of these additional questions and focus only on the star formation rate.

We develop our model in Sec. 2. In Sec. 3 we display examples of star formation rates we have computed for universes with different values of curvature, cosmological constant, and/or primordial density contrast. We identify important qualitative features that emerge in exotic regimes.

## 2. Model

### 2.1 Goals

Our goal is not a detailed analytical fit to simulations or observations of the SFR in our universe. Superior models are already available for this purpose. For example, the analytic model of Hernquist and Springel [4] (HS) contains some free parameters, tuned to yield good agreement with simulations and data. However, the HS model only allows for moderate variation in cosmological parameters. For example, HS estimated the SFR in cosmologies with different primordial density contrast,  $Q$ , but only by 10%.

Here we are interested in much larger variations, by orders of magnitude, and not only in  $Q$  but also in the cosmological constant,  $\Lambda$ , and in spatial curvature. A straightforward extrapolation of the HS model would lead to unphysical predictions in

some parameter ranges. For example, a larger cosmological constant would actually enhance the star formation rate at all times [5].<sup>1</sup>

In fact, important assumptions and approximations in the HS model become invalid under large variations of parameters. HS assume a fixed ratio between virial and background density. But in fact, the overdensity of freshly formed haloes drops from about 200 to about 16 after the cosmological constant dominates [6]. Moreover, HS apply a “fresh-halo approximation”, ascribing a virial density and star formation rate to each halo as if it had just been formed. However, large curvature, or a large cosmological constant, will disrupt the merging of haloes. One is left with an old population of haloes whose density was set at a much earlier time, and whose star formation may have ceased due to feedback or lack of baryons. Finally, HS neglect Compton cooling of virialized haloes against the cosmic microwave background; this effect becomes important if structure forms earlier, for example because of increased  $Q$  [7].

All these effects are negligible at positive redshift in our universe; they only begin to be important near the present era. Hence, there was no compelling reason to include them in conventional, phenomenologically motivated star formation models. But for different values of cosmological parameters, or when we study the entire evolution of the universe, these effects become important and must be modelled.

On the other hand, some aspects of star formation received careful attention in the HS model in order to optimize agreement with simulations. Such refinements are unnecessary when we work with huge parameter ranges, where uncertainties are large in any case. At best, our goal can be to gain a basic understanding of the quantitative behavior of the SFR as parameters are varied. We will mainly be interested in the height, time, and width of the peak of the SFR depend on parameters. In currently favored models of the multiverse [2, 8], more detailed aspects of the curve do not play an important role. Thus, our model will be relatively crude, even as we include qualitatively new phenomena.

Many extensions of our model are possible. The most obvious is to allow additional parameters to vary. Another is to refine the treatment of star formation itself. Among the many approximations and simplifications we make, the most significant may be our neglect of feedback effects from newly formed stars and from active galactic nuclei. In addition, there are two regimes in our model (high  $Q$  and negative  $\Lambda$  near the Big Crunch) where we use physical arguments to cut off star formation by hand. These are regimes where the star formation rate is so fast that neglected timescales, such as halo merger rates and star lifetimes, become important. An extended model which accounts for these timescales may avoid the need for an explicit cutoff.

---

<sup>1</sup>This effect, while probably unphysical, did not significantly affect the probability distributions computed by Cline *et al.* [5].

## 2.2 Geometry and initial conditions

Our star formation model can be applied to open, flat, and closed Friedman-Robertson-Walker (FRW) universes. However, we will consider only open geometries here, with metric

$$ds^2 = -dt^2 + a(t)^2 (d\chi^2 + \sinh^2 \chi d\Omega^2) . \quad (2.1)$$

Pocket universes produced by the decay of a false vacuum are open FRW universes [9]; thus, this is the case most relevant to a landscape of metastable vacua. The above metric includes the flat FRW case in the limit where the spatial curvature radius  $a$  is much larger than the horizon:

$$a \gg H^{-1} , \quad (2.2)$$

where  $H \equiv \dot{a}/a$  is the Hubble parameter. This can be satisfied at arbitrarily late times  $t$ , given sufficiently many  $e$ -foldings of slow roll inflation.

The scale factor,  $a(t)$ , can be computed by integrating the Friedmann equations,

$$H^2 - \frac{1}{a^2} = \frac{8\pi G_{\text{N}}}{3} \rho , \quad (2.3)$$

$$\dot{H} + H^2 = -\frac{4\pi G_{\text{N}}}{3}(\rho + 3p) , \quad (2.4)$$

beginning at (matter-radiation) equality, the time  $t_{\text{eq}}$  at which matter and radiation have equal density:

$$\rho_{\text{m}}(t_{\text{eq}}) = \rho_{\text{r}}(t_{\text{eq}}) \equiv \nu \frac{\pi^2}{15} T_{\text{eq}}^4 , \quad (2.5)$$

where

$$\nu = 1 + \frac{21}{8} \left( \frac{4}{11} \right)^{4/3} \approx 1.681 \quad (2.6)$$

accounts for three species of massless neutrinos. The temperature at equality is [6]

$$T_{\text{eq}} = 0.22\xi = 0.82 \text{ eV} , \quad (2.7)$$

and  $\xi$  is the matter mass per photon. The time of equality is

$$t_{\text{eq}} = \frac{\sqrt{2} - 1}{\sqrt{3\pi G_{\text{N}} \rho_{\text{m}}(t_{\text{eq}})}} \approx 0.128 G_{\text{N}}^{-1/2} T_{\text{eq}}^{-2} = 4.9 \times 10^4 \text{ yrs} . \quad (2.8)$$

The total density and pressure are given by

$$\rho = \rho_{\text{r}} + \rho_{\text{m}} + \rho_{\Lambda} , \quad (2.9)$$

$$p = \frac{\rho_{\text{r}}}{3} - \rho_{\Lambda} . \quad (2.10)$$

Among the set of initial data specified at equality, we will treat three elements as variable parameters, which define an ensemble of universes. The first two parameters are the densities associated with curvature,  $G_N^{-1}a(t_{\text{eq}})^{-2}$ , and with the vacuum,  $\rho_\Lambda \equiv \Lambda/8\pi G_N$ , at equality. We will only consider values that are small compared to the radiation and matter density at equality, Eq. (2.5); otherwise, there would be no matter dominated era and no star formation. The third parameter is the primordial density contrast,  $Q$ , discussed in more detail in the next section.

We find it intuitive to trade the curvature parameter  $a(t_{\text{eq}})$  for an equivalent parameter  $\Delta N$ , defined as

$$\Delta N = \log \left[ \frac{a(t_{\text{eq}})}{a_{\text{min}}(t_{\text{eq}})} \right], \quad (2.11)$$

where

$$a_{\text{min}}(t_{\text{eq}}) = \left( \frac{45 \Omega_m}{\nu 8\pi^3 G_N T_{\text{eq}}^4 H_0} \right)^{1/3} (\Omega_k^{\text{max}})^{-1/2} = 1.13 \times 10^{24} \text{ m} = 37 \text{ Mpc}, \quad (2.12)$$

is the experimental lower bound on the curvature radius of *our* universe at matter-radiation equality. (Consistency with our earlier assumption of an open universe requires that we use the upper bound on *negative* spatial curvature, i.e., on positive values of  $\Omega_k$ . We are using the 68% limit from WMAP5+BAO+SN [10],  $\Omega_k = -0.0050_{-0.0060}^{+0.0061}$ . We use the best fit values  $H_0 = 68.8 \text{ km/s/Mpc}$  and  $\Omega_m = 0.282$  for the current Hubble parameter and matter density fraction.)

$\Delta N$  can be interpreted as the number of  $e$ -folds of inflation in excess (or short) of the number required to make our universe (here assumed open) just flat enough ( $\Omega_k^{\text{max}} = 0.0011$ ) for its spatial curvature to have escaped detection. Requiring that curvature be negligible at equality constrains  $\Delta N$  to the range  $\Delta N > -5$ . Values near this cutoff are of no physical interest in any case: Because too much curvature disrupts galaxy formation, we will find that star formation already becomes totally ineffective below some larger value of  $\Delta N$ .

We hold fixed all other parameters, including Standard Model parameters, the baryon to dark matter ratio, and the temperature at equality. We leave the variation of such parameters to future work.

### 2.3 Linear perturbation growth and halo formation

Cosmological perturbations are usually specified by a time-dependent power spectrum,  $\mathcal{P}$ , which is a function of the wavenumber of the perturbation,  $k$ . The r.m.s. fluctuation amplitude,  $\sigma$ , within a sphere of radius  $R$ , is defined by smoothing the power spectrum

with respect to an appropriate window function:

$$\sigma^2 = \frac{1}{2\pi^2} \int_0^\infty \left( \frac{3 \sin(kR) - 3kR \cos(kR)}{(kR)^3} \right)^2 \mathcal{P}(k) k^2 dk . \quad (2.13)$$

The radius  $R$  can be exchanged for the mass  $M$  of the perturbation, using  $M = 4\pi\rho_m R^3/3$ . Starting at  $t_{\text{eq}}$ , once all relevant modes are in the horizon, the time development of  $\sigma$  can be computed using linear perturbation theory. In the linear theory, all modes grow at the same rate and so the time dependence of  $\sigma$  is a simple multiplicative factor:

$$\sigma(M, t) = Q s(M) G(t). \quad (2.14)$$

Here  $Q$  is the amplitude of primordial density perturbations, which in our universe is observed to be  $Q_0 \approx 2 \times 10^{-5}$ .  $G(t)$  is the linear growth function, and is found by solving

$$\frac{d^2 G}{dt^2} + 2H \frac{dG}{dt} = 4\pi G_N \rho_m G \quad (2.15)$$

numerically, with the initial conditions  $G = 5/2$  and  $\dot{G} = 3H/2$  at  $t = t_{\text{eq}}$ . This normalization is chosen so that  $G \approx 1 + \frac{3}{2} \frac{a(t)}{a(t_{\text{eq}})}$  near  $t = t_{\text{eq}}$ , which is the exact solution for a flat universe consisting only of matter and radiation. For  $s(M)$  we use the fitting formula provided in [6]:

$$s(M) = \left[ (9.1\mu^{-2/3})^{-0.27} + (50.5 \log_{10} (834 + \mu^{-1/3}) - 92)^{-0.27} \right]^{-1/0.27} \quad (2.16)$$

with  $\mu = M/M_{\text{eq}}$ , where

$$M_{\text{eq}} = G_N^{-3/2} \xi^{-2} = 1.18 \times 10^{17} M_\odot \quad (2.17)$$

is roughly the mass contained inside the horizon at equality, and  $\xi = 3.7$  eV is the matter mass per photon. This fitting formula for  $s(M)$  and our normalization convention for  $G(t)$  both make use of our assumption that curvature and  $\rho_\Lambda$  are negligible at  $t_{\text{eq}}$ .

We use the extended Press-Schechter (EPS) formalism [11] to estimate the halo mass function and the distribution of halo ages. In this formalism the fraction,  $F$ , of matter residing in collapsed regions with mass less than  $M$  at time  $t$  is given by

$$F(< M, t) = \text{Erf} \left( \frac{\delta_c}{\sqrt{2}\sigma(M, t)} \right) \quad (2.18)$$

with  $\delta_c = 1.68$  the critical fluctuation for collapse.  $\delta_c$  is weakly dependent on cosmological parameters, but the variation is small enough to ignore within our approximations.

Given a halo of mass  $M$  at time  $t$ , one can ask for the probability,  $P$ , that this halo virialized before time  $t_{\text{vir}}$ . As in Ref. [11], we define the virialization time of the

halo as the earliest time when its largest ancestor halo had a mass greater than  $M/2$ . To find  $P$ , we first define the function

$$\beta(M_1, t_1, M_2, t_2) = \text{Erfc} \left( \frac{\delta_c}{Q \sqrt{2(s(M_1)^2 - s(M_2)^2)}} \left( \frac{1}{G(t_1)} - \frac{1}{G(t_2)} \right) \right). \quad (2.19)$$

Then the desired probability is given by

$$P(< t_{\text{vir}}, M, t) = \int_{M/2}^M \frac{M}{M_1} \frac{d\beta}{dM_1}(M_1, t_{\text{vir}}, M, t) dM_1. \quad (2.20)$$

The virialization time further determines the density,  $\rho_{\text{vir}}$ , of the halo. We will compute the virial density by considering the spherical top-hat collapse of an overdense region of space. Birkhoff's theorem says that we may consider this region to be part of an independent FRW universe with a cosmological constant identical to that of the background universe. As such, it evolves according to

$$H^2 = \frac{8\pi G_{\text{N}} \rho_{\text{m}}}{3} + \frac{8\pi G_{\text{N}} \rho_{\Lambda}}{3} - \frac{k}{a^2} = \frac{8\pi G_{\text{N}} |\rho_{\Lambda}|}{3} \left( \frac{1}{A^3} \pm 1 - \frac{\kappa}{A^2} \right) \quad (2.21)$$

where  $A \equiv \left( \frac{|\rho_{\Lambda}|}{\rho_{\text{m}}} \right)^{1/3}$  and  $\kappa \equiv \frac{3}{8\pi G_{\text{N}} |\rho_{\Lambda}|} \left( \frac{A}{a} \right)^2 k$ . We neglect the radiation term, which will be negligible for virialization well after matter-radiation equality.

Assuming that  $\kappa$  and  $\rho_{\Lambda}$  are such that the perturbation will eventually collapse, the maximum value of  $A$  is obtained by solving the equation  $H = 0$ :

$$\pm A_{\text{max}}^3 - \kappa A_{\text{max}} + 1 = 0. \quad (2.22)$$

The time of collapse, which we identify with the halo virialization time  $t_{\text{vir}}$ , is twice the time to reach  $A_{\text{max}}$  and is given by

$$t_{\text{vir}} = 2 \sqrt{\frac{3}{8\pi G_{\text{N}} |\rho_{\Lambda}|}} \int_0^{A_{\text{max}}} \frac{dA}{\sqrt{\frac{1}{A} \pm A^2 - \kappa}}. \quad (2.23)$$

To obtain the virial density, we follow the usual rule that  $\rho_{\text{vir}}$  is 8 times the matter density at turnaround. In other words,

$$\rho_{\text{vir}} = 8 \frac{|\rho_{\Lambda}|}{A_{\text{max}}^3}. \quad (2.24)$$

Note that according to this prescription,  $\rho_{\text{vir}}(t)$  has no explicit dependence on the curvature of the background universe. Changing  $\rho_{\Lambda}$  results in a simple scaling behavior:  $\rho_{\text{vir}}(t/t_{\Lambda})/|\rho_{\Lambda}|$  is independent of  $\rho_{\Lambda}$ , where

$$t_{\Lambda} \equiv (3/8\pi G_{\text{N}} |\rho_{\Lambda}|)^{1/2}. \quad (2.25)$$

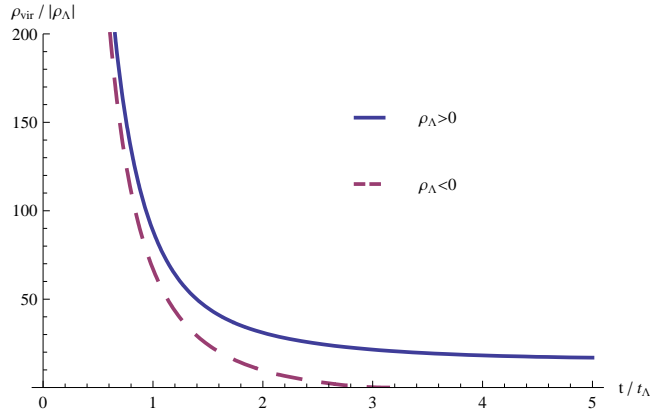


**Figure 1:** The virial density is independent of curvature and has a simple scaling dependence on  $\rho_\Lambda$ . For positive  $\rho_\Lambda$ ,  $\rho_{\text{vir}}$  asymptotes to  $16\rho_\Lambda$  at late times. For negative  $\rho_\Lambda$ , the virial density formally goes to zero at  $t = \pi t_\Lambda$ , which the latest possible time the universe can crunch. As we discuss in the text, our approximation (and, we shall assume, structure formation) fails when the virial density drops below the background matter density, which diverges near the crunch.

In practice this means that one only has to compute  $\rho_{\text{vir}}(t)$  for two values of  $\rho_\Lambda$  (one positive and one negative). In Fig. 1, we show the  $\rho_\Lambda$ -independent part of the virial density.

The virial density determines the gravitational timescale,  $t_{\text{grav}}$ , which we define to be

$$t_{\text{grav}} = \frac{1}{\sqrt{G_{\text{N}}\rho_{\text{vir}}}} . \quad (2.26)$$

This is the timescale for dynamical processes within the halo, including star formation.

## 2.4 Cooling and galaxy formation

Halos typically virialize at a high temperature,  $T_{\text{vir}}$ . Before stars can form, the baryons need to cool to lower temperatures and condense. Cooling proceeds by bremsstrahlung, molecular or atomic line cooling, and Compton cooling via scattering against the CMB.

For bremsstrahlung and line cooling, the timescale for the baryons to cool,  $t_{\text{cool}}$ , is

$$t_{\text{cool}} = \frac{3T_{\text{vir}}m_{\text{p}}^2}{2f_{\text{b}}\mu X^2\Lambda(T_{\text{vir}})\rho_{\text{vir}}} \quad (2.27)$$

with  $\mu = 0.6 m_{\text{p}}$  the average molecular weight (assuming full ionization),  $X = .76$  the hydrogen mass fraction, and  $\Lambda(T_{\text{vir}})$  the cooling function, which encodes the efficiency of the bremsstrahlung and line cooling mechanisms as a function of temperature. For  $T \lesssim 10^4$  K,  $\Lambda(T)$  is effectively zero and cooling does not occur. When  $T \gtrsim 10^7$  K,

bremsstrahlung cooling is the dominant mechanism and  $\Lambda(T) \propto T^{1/2}$ . For intermediate values of  $T$ ,  $\Lambda(T)$  has a complicated behavior depending on the metallicity of the gas [12]. For our purposes, however, it suffices to approximate the cooling function as constant in this range. To summarize:

$$\Lambda(T) = \begin{cases} 0, & \text{for } T < 10^4 \text{ K}, \\ \Lambda_0, & \text{for } 10^4 \text{ K} < T < 10^7 \text{ K}, \\ \Lambda_0 \left(\frac{T}{10^7 \text{ K}}\right)^{1/2}, & \text{for } 10^7 \text{ K} < T, \end{cases} \quad (2.28)$$

with  $\Lambda_0 = 10^{-23} \text{ erg cm}^3 \text{ s}^{-1}$ .

We need to include the effects of Compton cooling separately. In general, Compton cooling depends on the temperature of the CMB,  $T_{\text{CMB}}$ , the temperature of the baryonic matter, and the ionization fraction of the matter [13]. But the dependence on the gas temperature drops out when  $T_{\text{vir}} \gg T_{\text{CMB}}$  (which is always the case), and we will assume that the gas transitions from neutral to completely ionized at  $T_{\text{vir}} = 10^4 \text{ K}$ . With these approximations, Compton cooling proceeds along the timescale

$$t_{\text{comp}} = \frac{45m_e}{4\pi^2\sigma_{\text{T}}(T_{\text{CMB}})^4}, \quad (2.29)$$

where  $\sigma_{\text{T}} = \frac{8\pi}{3} \left(\frac{e^2}{m_e}\right)^2$  is the Thompson cross-section.

The Compton timescale is independent of all of the properties of the gas (provided  $T_{\text{vir}} > 10^4 \text{ K}$ ). So this cooling mechanism can still be efficient in regimes where other cooling mechanisms fail. In particular, Compton cooling will be extremely effective in the early universe while the CMB is still hot. We define  $\tau_{\text{comp}}$  as the time when  $t_{\text{comp}}$  is equal to the age of the universe.  $\tau_{\text{comp}}$  is a reasonable convention for the time beyond which Compton cooling is no longer efficient. While we compute  $\tau_{\text{comp}}$  numerically in practice, it is helpful to have an analytic formula for a special case. In a flat,  $\rho_{\Lambda} = 0$  universe we obtain

$$\tau_{\text{comp}} = \left(\frac{4\pi^2\sigma_{\text{T}}(T_{\text{eq}})^4}{45m_e} \left(\frac{t_{\text{eq}}}{2 - \sqrt{2}}\right)^{8/3}\right)^{3/5} \approx 0.763 \left(\frac{T_{\text{eq}}}{\text{eV}}\right)^{-4/5} \text{ Gyr} \approx 0.9 \text{ Gyr}. \quad (2.30)$$

Turning on strong curvature or  $\rho_{\Lambda}$  will tend to lower  $\tau_{\text{comp}}$ .

Before  $\tau_{\text{comp}}$ , all structures with  $T_{\text{vir}} > 10^4 \text{ K}$  can cool efficiently and rapidly, so star formation will proceed on the timescale  $t_{\text{grav}}$ . After  $\tau_{\text{comp}}$ , some halos will have  $t_{\text{cool}} < t_{\text{grav}}$  and hence cool efficiently, and some will have  $t_{\text{cool}} > t_{\text{grav}}$  and be “cooling-limited”. We take it as a phenomenological fact that the cooling-limited halos do not form stars. (One could go further and define a “cooling radius” to take into account

the radial dependence of the baryonic density [13], but this effect is negligible within our approximations.)

In the absence of Compton cooling, then, we will consider only halos for which  $t_{\text{cool}} < t_{\text{grav}}$ , which have masses in a finite range:

$$M_{\text{min}}(t_{\text{vir}}) < M < M_{\text{max}}(t_{\text{vir}}) . \quad (2.31)$$

The minimum halo mass at time  $t_{\text{vir}}$  corresponds to the minimum temperature  $T_{\text{vir}} = 10^4\text{K}$ :

$$M_{\text{min}}(t_{\text{vir}}) = \left( \frac{5 \times 10^4 \text{ K}}{G_{\text{N}} \mu} \right)^{3/2} \left( \frac{3}{4\pi \rho_{\text{vir}}} \right)^{1/2} , \quad (2.32)$$

where we have used the relation between virial temperature, density, and mass for a uniform spherical halo derived from the virial theorem:

$$T_{\text{vir}} = \frac{G_{\text{N}} \mu}{5} \left( \frac{4\pi}{3} \rho_{\text{vir}} M^2 \right)^{1/3} . \quad (2.33)$$

(A non-uniform density profile will result in a change to the numerical factor on the RHS of this equation, but such a change makes little difference to the result.)

The maximum mass haloes at time  $t_{\text{vir}}$  satisfy  $t_{\text{cool}} = t_{\text{grav}}$ . For  $T < 10^7\text{K}$ , this mass is given by

$$M_{\text{max}}(t_{\text{vir}}) = \left( \frac{6}{\pi} \right)^{1/2} \left( \frac{5 f_{\text{b}} X^2 \Lambda_0}{3 G_{\text{N}}^{3/2} m_{\text{p}}^2} \right)^{3/2} \rho_{\text{vir}}^{1/4} . \quad (2.34)$$

Note that halos with mass  $M_{\text{max}}(t)$  have virial temperatures less than  $10^7\text{K}$  for  $t \gtrsim 0.24 \text{ Gyr}$ , which is well before  $\tau_{\text{comp}}$ . This means that in our calculations we can safely ignore the decreased cooling efficiency for extremely hot halos.

## 2.5 Star formation

For halos satisfying the criterion  $t_{\text{cool}} < t_{\text{grav}}$ , the hot baryonic material is allowed to cool. Gravitational collapse proceeds on the longer timescale  $t_{\text{grav}}$ . We will assume that the subsequent formation of stars is also governed by this timescale. Thus, we write the star formation rate for a single halo of mass  $M$  as

$$\frac{dM_{\star}^{\text{single}}}{dt}(M, t_{\text{vir}}) = A \frac{M_{\text{b}}}{t_{\text{grav}}(t_{\text{vir}})} = A \frac{f_{\text{b}} M}{t_{\text{grav}}(t_{\text{vir}})} , \quad (2.35)$$

where  $M_{\text{b}}$  is the total mass of baryons contained in the halo and  $f_{\text{b}}$  is the baryon mass fraction. We fix  $f_{\text{b}}$  to the observed value  $f_{\text{b}} \approx 1/6$ .<sup>2</sup>

---

<sup>2</sup>It would be interesting to consider variations of  $f_{\text{b}}$  in future work; see Ref. [14] for an environmental explanation of the observed value.

The order-one factor  $A$  parametrizes the detailed physics of gravitational collapse and star formation. The free-fall time from the virial radius to a point mass  $M$  is  $(3\pi/32)^{1/2} t_{\text{grav}}$ , and so we choose to set  $A = (32/3\pi)^{1/2}$ . The final SFR calculated for our universe is not very sensitive to this choice. Notice that the single halo star formation rate depends only on the mass and virialization time of the halo.

The next step in computing the complete SFR is to average over the virialization times of the halos in existence at time  $t$ . Define  $\frac{dM_{\star}^{\text{avg}}}{dt}(M, t)$  to be the star formation rate of all halos that have mass  $M$  at time  $t$ , averaged over possible virialization times  $t_{\text{vir}}$ . Now we need to consider the possible virialization times.

It may happen that some halos in existence at time  $t$  are so old that they have already converted all of their baryonic mass into stars. These halos should not be included in the calculation. Furthermore, feedback effects reduce the maximum amount of baryonic matter that can ever go into stars to some fraction  $f$  of the total. ( $f$  is a free parameter of the model, and we shall fix its value by normalizing the integrated SFR for our universe; see below.) We should then only consider halos with  $t_{\text{vir}} > t_{\text{min}}$ , where  $t_{\text{min}}$  is a function of  $t$  only and satisfies

$$t - t_{\text{min}} = \left( \frac{1}{fM_{\text{b}}} \frac{dM_{\star}^{\text{single}}}{dt}(M, t_{\text{min}}) \right)^{-1} = \frac{f}{A} t_{\text{grav}}(t_{\text{min}}) . \quad (2.36)$$

Though an explicit expression for  $t_{\text{min}}$  can be found in some special cases, in practice we will always solve for it numerically.

We still need to account for the fact that some halos existing at  $t$  formed at  $t_{\text{vir}}$  with masses outside the range  $M_{\text{min}}(t_{\text{vir}}) < M < M_{\text{max}}(t_{\text{vir}})$ . Since  $M_{\text{min}}$  is an increasing function of time while  $M_{\text{max}}$  is a decreasing function of time, this condition on the mass range is equivalent to an upper bound on  $t_{\text{vir}}$ :  $t_{\text{vir}} < t_{\text{max}}$ , where  $t_{\text{max}}$  satisfies either

$$M = M_{\text{max}}(t_{\text{max}}) \quad (2.37)$$

or

$$M = M_{\text{min}}(t_{\text{max}}) , \quad (2.38)$$

or else  $t_{\text{max}} = t$  if no solution exists. Recall that the condition  $M < M_{\text{max}}$  is a condition on cooling failure, and so is only applicable for  $t_{\text{vir}} > \tau_{\text{comp}}$ . Halos with  $t_{\text{vir}} < \tau_{\text{comp}}$  have no upper mass limit. Like  $t_{\text{min}}$ ,  $t_{\text{max}}$  is found numerically. Unlike  $t_{\text{min}}$ ,  $t_{\text{max}}$  is a function of both mass and time.

Now we can use the distribution on halo formation times deduced from Eq. 2.20 to get

$$\frac{dM_{\star}^{\text{avg}}}{dt}(M, t) = \int_{t_{\text{min}}}^{t_{\text{max}}} \left[ \frac{Af_{\text{b}}M}{t_{\text{grav}}(t_{\text{vir}})} \frac{\partial P}{\partial t_{\text{vir}}}(t_{\text{vir}}, M, t) \right] dt_{\text{vir}} . \quad (2.39)$$

The final step is to multiply this average by the number of halos of mass  $M$  existing at time  $t$  and add up the contributions from all values of  $M$ . Equivalently, we can multiply the normalized average star formation rate,  $\frac{1}{M} \frac{dM_*^{\text{avg}}}{dt}$ , by the total amount of mass in halos of mass  $M$  at time  $t$  and then add up the contributions from the different mass scales. The Press-Schechter formalism tells us that the fraction of the total mass contained in halos of masses between  $M$  and  $M + dM$  is  $\frac{\partial F}{\partial M} dM$ , where  $F(M, t)$  is the Press-Schechter mass function defined in Eq. 2.18. So restricting ourselves to a unit of comoving volume with density  $\rho_0$  (sometimes called the reference density), we find that the SFR is given by

$$\dot{\rho}_*(t) = \rho_0 \int dM \int_{t_{\min}}^{t_{\max}} dt_{\text{vir}} \frac{\partial F}{\partial M}(M, t) \frac{A f_b}{t_{\text{grav}}(t_{\text{vir}})} \frac{\partial P}{\partial t_{\text{vir}}}(t_{\text{vir}}, M, t). \quad (2.40)$$

**Normalizing the SFR** Our model contains the free parameter  $f$  representing the maximum fraction of the total baryonic mass of a halo which can go into stars. We will impose a normalization condition on the SFR for our universe to fix its value. Nagamine *et al.* [15] normalize their “fossil” SFR so that

$$\int_0^{t_0} \dot{\rho}_* dt = \frac{f_b \rho_m}{10}, \quad (2.41)$$

with  $t_0 = 13.7 \text{ Gyr}$  the age of the universe. In other words, the total amount of mass going into stars should be one tenth of the total baryonic mass in the universe. Due to the phenomenon of recycling, this number is more than the actual amount of matter presently found in stars. We find that with  $f = 0.35$ , our model satisfies this normalization condition.

**Early and late time cutoffs** Even after  $t = t_{\text{eq}}$ , baryonic matter remains coupled to photons until  $t = t_{\text{rec}} \approx 3.7 \times 10^5 \text{ yr}$ . So even though dark matter halos can and do begin to collapse before recombination, stars will obviously be unable to form. After  $t = t_{\text{rec}}$ , the baryons are released and will fall into the gravitational wells of the pre-formed dark matter halos. Some time  $\Delta t$  (of order  $t_{\text{rec}}$ ) later, the baryonic matter will have fallen into the dark matter halos and can form stars normally. In our model, we account for this effect by placing further conditions on  $t_{\min}$ . First, if  $t < 2 t_{\text{rec}}$  then the SFR is set to zero. Then, provided  $t > 2 t_{\text{rec}}$ , we compute  $t_{\min}$  according to Eq. 2.36. If we find that  $t_{\min} < 2 t_{\text{rec}} < t$ , then the computation of  $t_i$  is flawed and we set  $t_{\min} = t_{\text{eq}}$  to reflect the fact that dark matter halos have been growing since equality. If  $t_{\min} > 2 t_{\text{rec}}$ , then the computation is valid and we keep the result.

For  $\rho_\Lambda < 0$  there is an additional cutoff we must impose. One can see from Fig. 1 that halo virial density in such a universe continually decreases over time even as the

background matter density increases (following turnaround). Eventually we reach a point where halos virialize with densities less than that of the background, which is a signal of the breakdown of the spherical collapse model.

The problem is that formally, the virial radius of the halo is larger than the radius of the “hole” that was cut out of the background and which is supposed to contain the “overdensity”. Thus, virialization really leads to a collision with the background, and not to a star forming isolated halo. Physically, this can be interpreted as a breakdown of the FRW approximation: sufficiently close to the crunch, the collapsing universe can no longer be sensibly described as homogeneous on average.

Therefore, it makes sense to demand that the halo density be somewhat larger than the background density. To pick a number, we assume that under normal circumstances, a halo would settle into an isothermal configuration with a density proportional to  $1/r^2$ . Therefore the density on the edge of the halo will only be one third of the average density. If we demand a reasonable separation of scales between the density of the halo edge and that of the background matter, an additional factor of about 3 is not uncalled for. So we will impose the requirement that the average density of the halo be a factor of ten higher than the background matter density.

We set the SFR to zero in any halos which do not satisfy this requirement. We implement this through a modification of the computation of  $t_{\text{max}}$ . The true  $t_{\text{max}}$ , computed at time  $t$ , is actually the minimum of the result above (Eqs. 2.37–2.38) and the solution to

$$\rho_{\text{vir}}(t_{\text{max}}) = 10 \rho_{\text{m}}(t) . \quad (2.42)$$

### 3. Results

In this section, we apply our model to estimate the star formation rate, and the integrated amount of star formation, in universes with various amounts of curvature, vacuum energy, and density contrast.

#### 3.1 Our universe

We begin by considering our own universe. Figure 2 shows the SFR computed by our model as a function of time (left) and of redshift (right). At intermediate redshifts, our model is in good agreement with the data. At other redshifts, our model appears to be slightly off, but not by a large factor, considering its crudeness. For comparison, we show the SFR predicted by the models of HS [4], Nagamine *et al.* [15] and Hopkins and Beacom [16], which contain a larger number of fitting parameters.

The shape of the SFR can be understood as a result of the interplay between competing forces. First, there will be no star formation until structure forms with

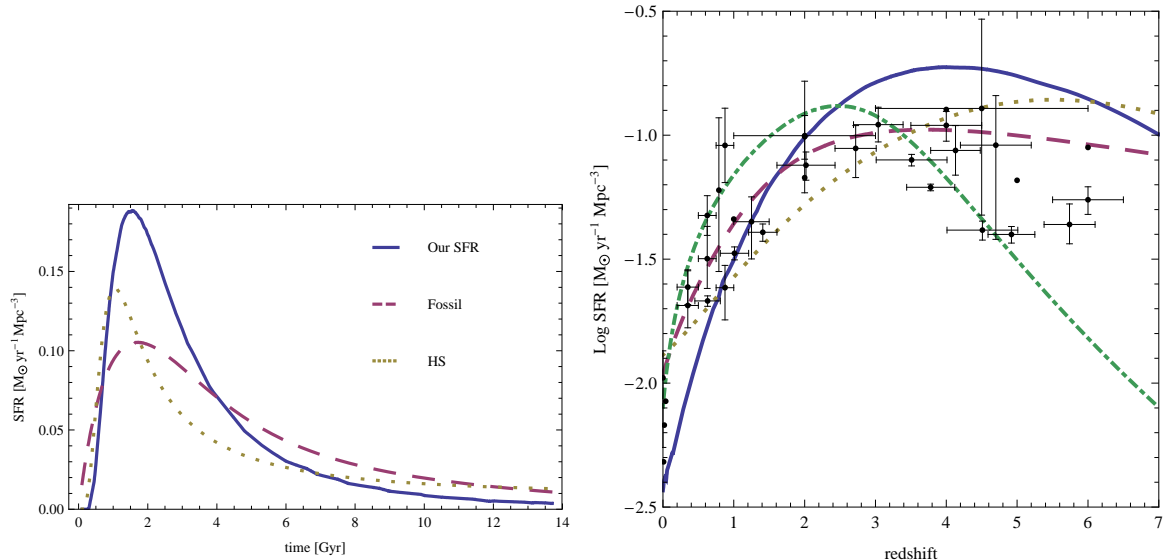


**Figure 2:** Comparison of our calculated SFR (solid) with the fossil model of Nagamine *et al.* [15] (dashed) and the HS model [4] (dotted). The right plot contains, in addition, the SFR of Hopkins and Beacom [16] (dash-dotted). The data points in the right plot are from astronomical observations and were compiled, along with references to their original sources, in [15]

$T_{\text{vir}} > 10^4 \text{K}$ . Once a significant amount of structure begins to form at this critical temperature, however, the SFR rises rapidly and soon hits its peak.

We can estimate the peak time,  $t_{\text{peak}}$ , of the SFR by asking when the typical mass scale that virializes is equal to  $M_{\text{min}}$ :

$$\frac{\delta_c}{\sqrt{2}\sigma(M_{\text{min}}(t_{\text{peak}}), t_{\text{peak}})} = 1 . \quad (3.1)$$

(There are ambiguities at the level of factors of order one; the factor  $\sqrt{2}$  was chosen to improve agreement with the true peak time of the SFR.) For the parameters of our universe, this calculation yields  $t_{\text{peak}} = 1.7 \text{Gyr}$ , close to the peak predicted by our model at about 1.6 Gyr.

After  $t \approx t_{\text{peak}}$ , the SFR falls at least as fast as  $1/t$  because  $t_{\text{grav}} \propto t$ . Once the typical virialized mass exceeds the cooling limit,  $M_{\text{max}}$ , the SFR falls faster still. These considerations generalize to universes besides our own after accounting for the peculiar effects of each of the cosmological parameters. In particular, as explained below, we should be able to accurately estimate the peak time by this method for any universe where the effects of curvature or the cosmological constant are relatively weak.

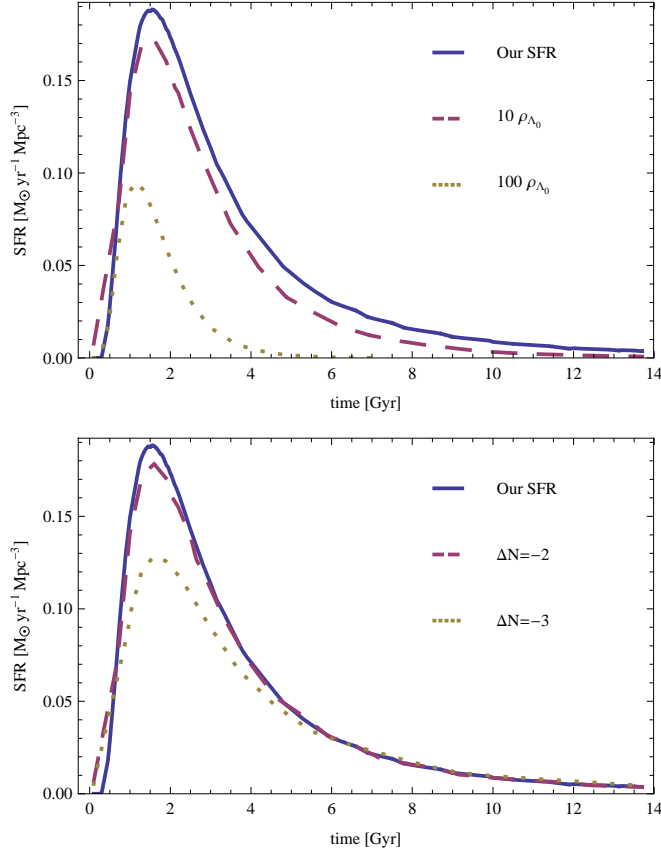


**Figure 3:** The SFR for universes with greater cosmological constant (top) and more curvature (bottom) than ours. All other parameters remain fixed to the observed values, with curvature assumed to be open and just below the observational bound.

### 3.2 Varying single parameters

Next, we present several examples of star formation rates computed from our model for universes that differ from ours through a single parameter.

**Curvature and positive cosmological constant** In Fig. 3, we show the SFR for our universe together with the SFRs computed for larger values of the cosmological constant (top) and larger amounts of curvature (bottom). One can see that increasing either of these two quantities results in a lowered star formation rate.<sup>3</sup> Essentially

---

<sup>3</sup>This differs from the conclusions obtained by Cline *et al.* [5] from an extrapolation of the Hernquist-Springel analytical model [4]. This model approximates all haloes in existence at time  $t$  as freshly formed. Moreover, it does not take into account the decreased relative overdensity of virialized haloes in a vacuum-dominated cosmology. These approximations are good at positive redshift in our universe, but they do not remain valid after structure formation ceases.

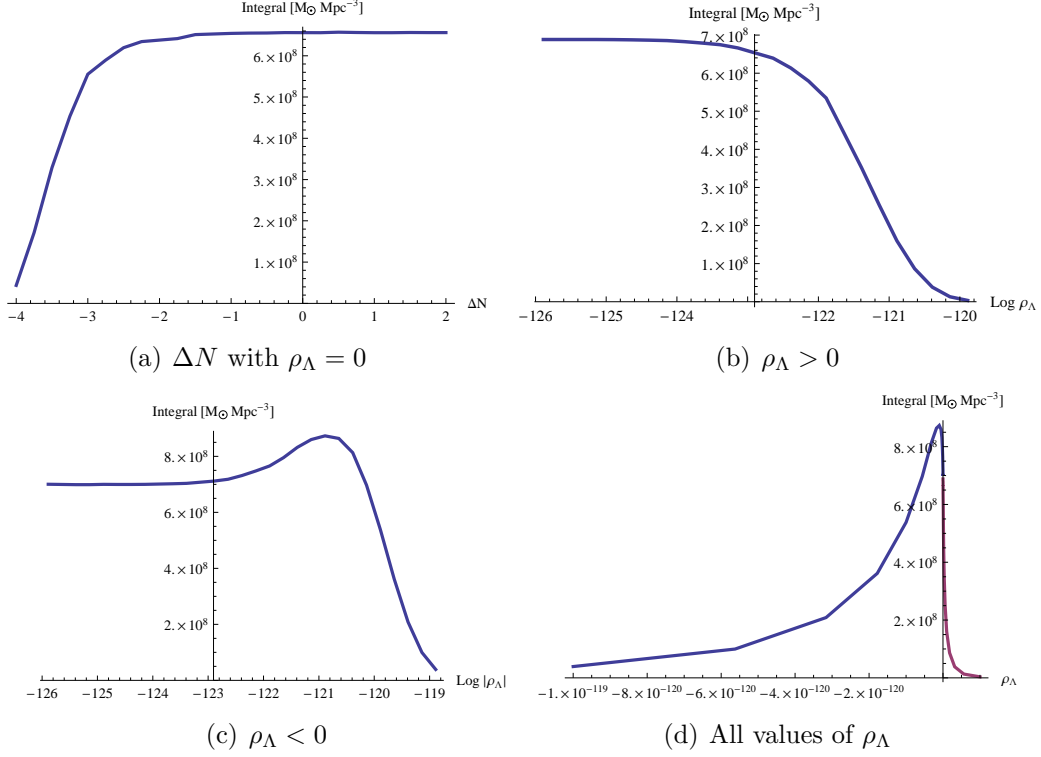


**Figure 4:** The total stellar mass produced per comoving volume, as a function of open spatial curvature and the cosmological constant. (a) Curvature: Integrated SFR as a function of the number of e-folds of inflation, relative to the observational bound on open spatial curvature. For  $\Delta N \gtrsim -2$ , star formation is unaffected. More curvature (less inflation) suppresses star formation, as expected. (The small irregularities in the asymptotic regime are numerical artifacts.) (b) Positive cosmological constant:  $\rho_\Lambda$  is given in Planck units; the observed value,  $\rho_{\Lambda_0} \approx 1.25 \times 10^{-123}$ , is indicated by the position of the vertical axis. Decreasing  $\rho_\Lambda$  has no effect on star formation. Larger values interfere with structure formation, and star formation becomes suppressed. (c) Negative cosmological constant: Enhanced structure formation leads to more star formation for negative vacuum energy compared to positive vacuum energy of equal magnitude. (d) Positive and negative values of the cosmological constant shown on a linear plot.

this is because structure formation as a whole is inhibited in these universes. Star formation is obstructed by the cosmological constant starting at the time  $t \sim t_\Lambda \equiv (3/\Lambda)^{1/2}$ . Open spatial curvature suppresses star formation after the time of order  $t_c = 0.533 \frac{8\pi}{3} \rho_{\text{eq}} a(t_{\text{eq}})^3$ , when  $\Omega = 0.5$  in an open universe with  $\rho_\Lambda = 0$ . Not shown are SFRs from universes which have a smaller cosmological constant than our universe, nor universes that are more spatially flat than the observational bound ( $\Delta N > 0$ ). The SFRs for those choices of parameters are indistinguishable from the SFR for our

universe.

In Fig. 4(a), the integrated star formation rate is shown as a function of  $\Delta N$ . It is apparent that extra flatness beyond the current experimental bound does not change star formation. Indeed, the curve remains flat down to about  $\Delta N \approx -2$ , showing that the universe could have been quite a bit more curved without affecting star formation. Integrated star formation is suppressed by a factor 2 for  $\Delta N = -3.5$  and by a factor 10 for  $\Delta N = -4$ .

These numbers differ somewhat from the catastrophic boundary used in Ref. [17],  $\Delta N = -2.5$ . This is because the observational upper bound on  $\Omega_k$  has tightened from the value  $20 \times 10^{-3}$  used in Ref. [17] to  $1.1 \times 10^{-3}$ . The observationally allowed region corresponds to  $\Delta N \geq 0$ . Future probes of curvature are limited by cosmic variance to a sensitivity of  $\Omega_k \gtrsim 10^{-4}$  or worse, corresponding to  $\Delta N \lesssim 1$  at most. The window for discovery of open curvature has narrowed, but it has not closed.

The string landscape predicts a non-negligible probability for a future detection of curvature in this window. (This prediction is contingent on cosmological measures which do not reward volume expansion factors during slow-roll inflation, such as the causal diamond measure [2] or the scale factor measure [8]; such measures are favored for a number of reasons.) Depending on assumptions about the underlying probability distribution for  $\Delta N$  in the landscape (and on the details of the measure), this probability may be less than 1% or as much as 10% [18]. However, the fact that curvature is already known to be much less than the anthropic bound makes it implausible to posit a strong landscape preference for small  $\Delta N$ , making a future detection rather unlikely.

In Fig. 4(b), the integrated star formation rate is shown as a function of (positive)  $\rho_\Lambda$ . The observed value of  $\rho_\Lambda$  is right on the edge of the downward slope, where vacuum energy is beginning to affect star formation. Integrated star formation is suppressed by a factor 2 for  $\rho_\Lambda = 36\rho_{\Lambda_0}$  and by a factor 10 for  $\rho_\Lambda = 225\rho_{\Lambda_0}$ . To obtain a probability distribution for  $\rho_\Lambda$  from this result, one needs to combine it with a cosmological measure [18].

**Negative cosmological constant** In Fig. 5 we see the SFR in some universes with negative cosmological constant. It is instructive to compare universes that differ only through the sign of the cosmological constant. The universe with negative vacuum energy will eventually reach a Big Crunch, where star formation ends along with everything else. Yet, it will generally have a greater star formation rate than its partner with positive vacuum energy. This is because in the positive case, structure formation is severely hindered as soon as vacuum energy comes to dominate, at  $t \approx t_\Lambda$ , due to the exponential growth of the scale factor. In the negative case, this timescale roughly corresponds to the turnaround. Structure formation not only continues during this

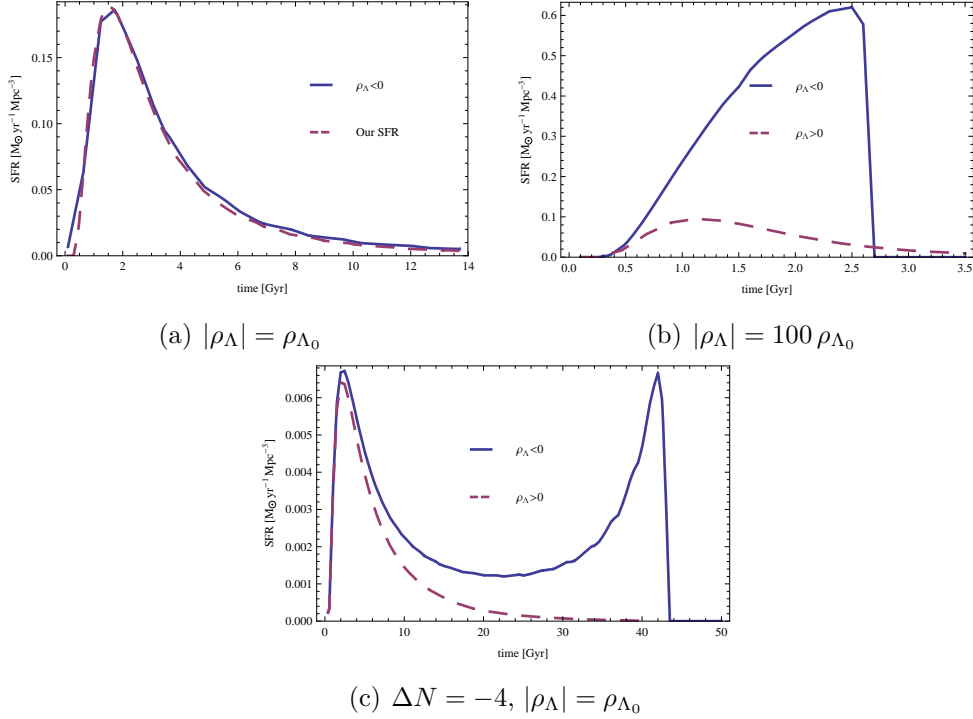


**Figure 5:** The SFR with negative cosmological constant. In each figure we consider two different universes whose parameters are identical except for the sign of  $\rho_\Lambda$ . (a) Changing the sign of the observed cosmological constant would have made little difference to the SFR. However, in universes with a higher magnitude of cosmological constant (b), or more highly curved universes (c), a negative cosmological constant allows more star formation than a positive one of equal magnitude. The apparent symmetry in (c) is accidental.

phase and during the early collapse phase, but is enhanced by the condensation of the background. Star formation is eventually cut off by our requirement that the virial density exceed the background density by a sufficient factor, Eq. (2.42). This is the origin of the precipitous decline in Fig. 5(b) and (c).

The integrated star formation rate as a function of negative values of the cosmological constant is shown in Fig. 4. As in the positive case, sufficiently small values of  $|\rho_\Lambda|$  do not affect star formation. A universe with large negative  $\rho_\Lambda$  will crunch before stars can form. For intermediate magnitudes of  $\rho_\Lambda$ , there is more star formation in negative than in positive cosmological constant universes. The amount of this excess is quite sensitive to our cutoff prescription near the crunch, Eq. (2.42). With a more lenient cutoff, there would be even more star formation in the final collapse phase. A stronger cutoff, such as the condition that  $\rho_{\text{vir}} > 100 \rho_m$ , would eliminate the excess entirely. Clearly, a more detailed study of structure and star formation in collapsing

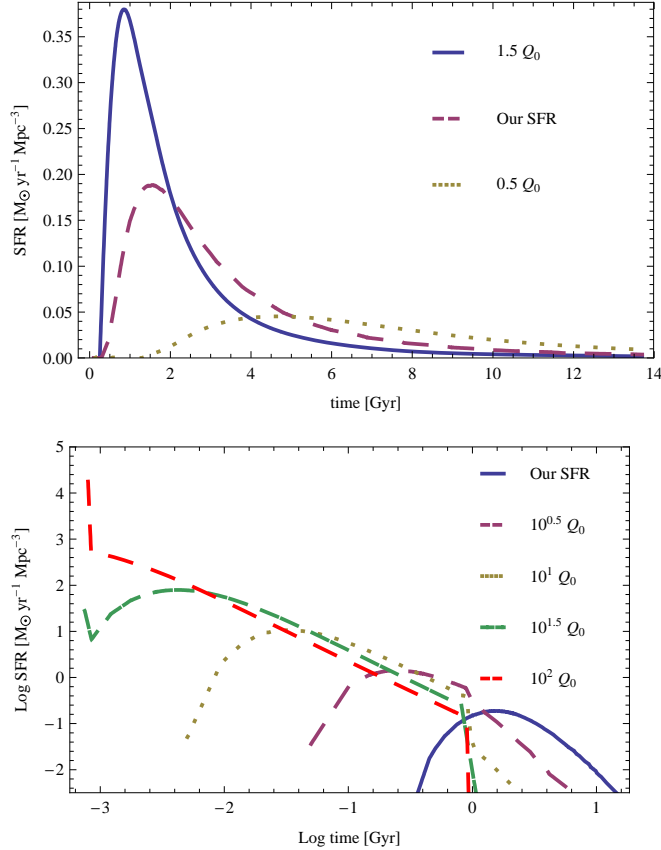


**Figure 6:** The SFR for different values of the primordial density contrast,  $Q$ . The upper plot shows the great sensitivity of the SFR to relatively small changes in  $Q$ . Compton cooling plays no role here. The lower plot shows a larger range of values. The universal slope of  $-1$  in the log-log plot corresponds to the  $1/t$  drop-off in the Compton cooling regime. When Compton cooling becomes ineffective at around 1 Gyr, most of the SFRs experience a sudden drop. The spike at early times for large values of  $Q$  arises from the sudden influx of baryons after recombination.

universes would be desirable.

**Density contrast** In Fig. 6 we see the effect of increasing or decreasing the amplitude of primordial density perturbations,  $Q$ . Note that even relatively small changes in  $Q$  have a drastic impact on the SFR. Increasing  $Q$  has the effect of accelerating structure formation, thus resulting in more halos forming earlier. Earlier formation times mean higher densities, which in turn means higher star formation rates.

Of course, higher  $Q$  also leads to larger halo masses. One might expect that cooling becomes an issue in these high-mass halos, and indeed for high values of  $Q$  the SFR

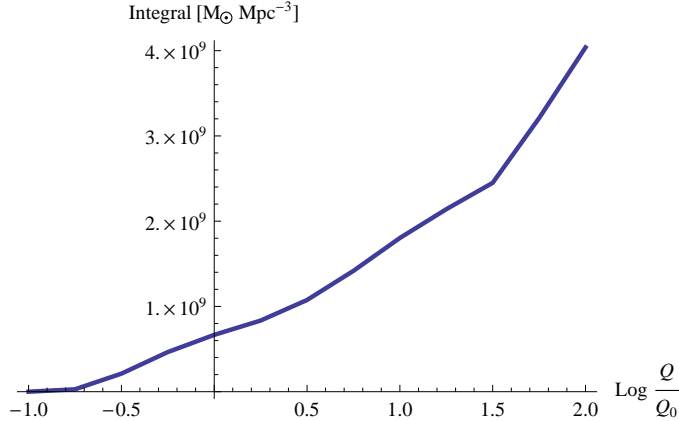


**Figure 7:** In our model, total star formation increases with the density contrast. This increase continues until we can no longer trust our SFR due to the dominance of large-scale structure at recombination. As discussed in the text, a more refined model may find star formation inhibited in parts of the range shown here.

drops to zero once Compton cooling fails, at  $t = \tau_{\text{comp}}$ . However, for  $t < \tau_{\text{comp}}$ , cooling does not limit star formation, and so in high  $Q$  universes there tends to be a very large amount of star formation at early times. For the highest values of  $Q$  that we consider, there is a spike in the star formation rate at  $t = 2 t_{\text{rec}}$  coming from the sudden infall of baryons to the dark matter halos. The spike is short-lived and disappears once that initial supply of gas is used up.

In Fig. 7 we show the integral of the SFR as a function of  $Q$ . The increase in total star formation is roughly logarithmic, and in our model the increase keeps going until most structure would form right at recombination, which signals a major regime change and a likely breakdown of our model.

A universe with high  $Q$  is a very different place from the one we live in: the densities and masses of galaxies are both extremely high. It is possible that qualitatively new phenomena, which we are not modelling, suppress star formation in this regime. For example, no detailed study of cooling flows, fragmentation, and star formation in the Compton cooling regime has been performed. We have also neglected the effects of enhanced black hole formation.

### 3.3 Varying multiple parameters

We can also vary multiple parameters at once. For example, let us hold only  $Q$  fixed and vary both curvature and (positive) vacuum energy. The integrated star formation is shown in Fig. 8. If either curvature or  $\rho_\Lambda$  get large, then structure formation is suppressed and star formation goes down. When the universe has both small  $\rho_\Lambda$

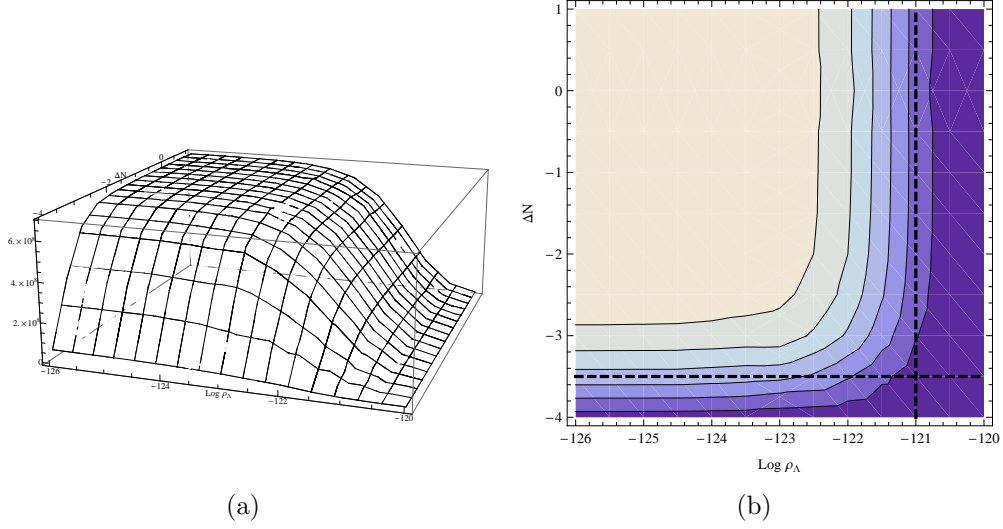


**Figure 8:** The integrated SFR as a function of curvature ( $\Delta N$ ) and positive  $\rho_\Lambda$ , shown in a 3D plot (a) and in a contour plot (b). (The strength of density perturbations,  $Q$ , is fixed to the observed value.) Analytically one expects star formation to be suppressed if  $t_{\text{peak}} > t_c$  or  $t_{\text{peak}} > t_\Lambda$ , where  $t_{\text{peak}}$  is the peak star formation time in the absence of vacuum energy and curvature. These catastrophic boundaries,  $\log_{10} \rho_\Lambda = -121$  and  $\Delta N = -3.5$ , are shown in (b).

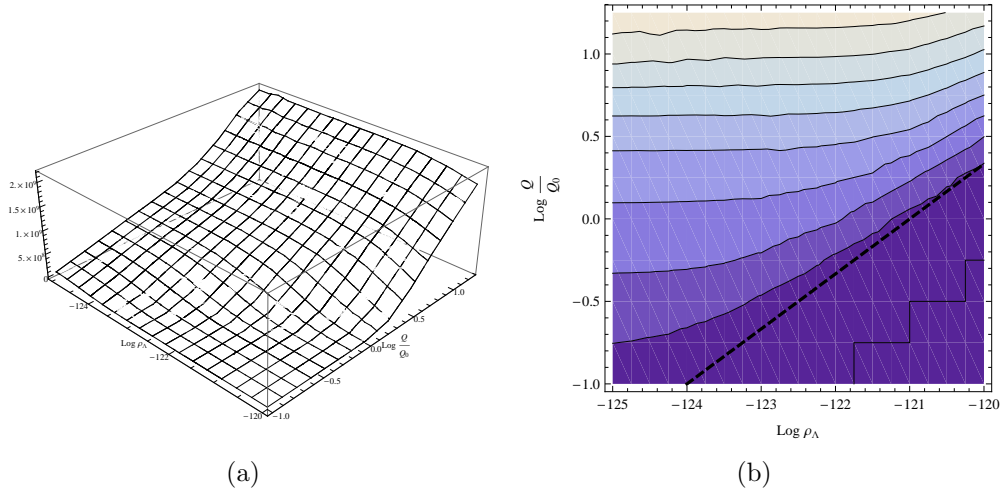


**Figure 9:** The integrated SFR as a function of positive  $\rho_\Lambda > 0$  and  $Q$ , at fixed spatial curvature,  $\Delta N = 0$ . The contour plot (b) also shows the catastrophic boundary  $t_{\text{peak}}(Q) > t_\Lambda$  expected analytically.

and small curvature, then structure formation is not suppressed and the SFR is nearly identical to that of our universe. Here “large” and “small” should be understood in

terms of the relation between  $t_\Lambda$ ,  $t_c$ , and  $t_{\text{peak}}$  computed in a flat,  $\rho_\Lambda = 0$  universe (an unsuppressed universe). In the case we are considering, namely  $Q = Q_0$ , the unsuppressed peak time is  $t_{\text{peak}} = 1.7$  Gyr. The conditions  $t_{\text{peak}} = t_\Lambda$  and  $t_{\text{peak}} = t_c$  translate into  $\rho_\Lambda \approx 100 \rho_{\Lambda_0}$  and  $\Delta N \approx -3.5$ . These lines are marked in Fig. 8(b), and one sees that this is a good approximation to the boundary of the star-forming region. (We will see below that this approximation does not continue to hold if both curvature and  $Q$  are allowed to vary.)

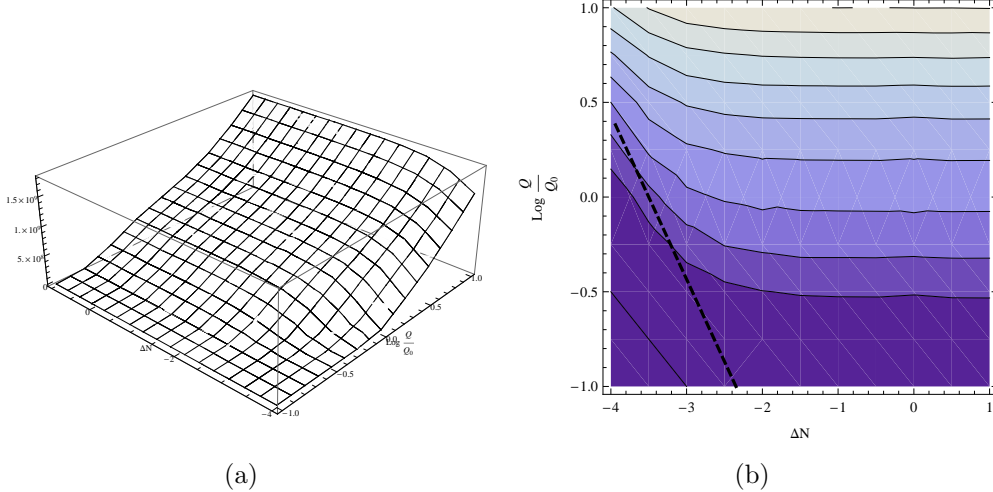


**Figure 10:** The integrated SFR as a function of  $\Delta N$  and  $Q$ , at fixed  $\rho_\Lambda = \rho_{\Lambda_0}$ . The contour plot (b) also shows the boundary  $t_{\text{peak}}(Q) > t_c$  expected analytically, but this analytic boundary is not a good approximation to the true catastrophic boundary.

If we also start to vary  $Q$ , the story gets only slightly more complicated. Increasing  $Q$  causes structure formation to happen earlier, resulting in more star formation. In the multivariate picture, then, it is helpful to think of  $Q$  as changing the unsuppressed  $t_{\text{peak}}$ . For the unsuppressed case, the universe can be approximated as matter-dominated. Looking at Eq. 3.1 and recalling that  $G \sim a \propto t^{2/3}$  in a matter-dominated universe, and neglecting for the sake of computational ease the dependence on  $M_{\text{min}}$ , we see that  $t_{\text{peak}} \propto Q^{-3/2}$ . Now we can quantitatively assess the dependence of star formation on  $Q$  and  $\rho_\Lambda$ , for instance. We know that  $t_\Lambda = t_{\text{peak}}$  when  $Q = Q_0$  and  $\rho_\Lambda = 100 \rho_{\Lambda_0}$ , and this condition should generally mark the boundary between star formation and no star formation. Therefore we can deduce that the boundary in the two-dimensional parameter space is the line  $\log_{10} \rho_\Lambda / \rho_{\Lambda_0} = 2 + 3 \log_{10} Q / Q_0$ . This line is shown in Fig. 9(b), where it provides a good approximation to the failure of star formation.

We can repeat the same analysis for the case of fixed cosmological constant with varying curvature and perturbation amplitude. In Fig. 10 we show the integrated star

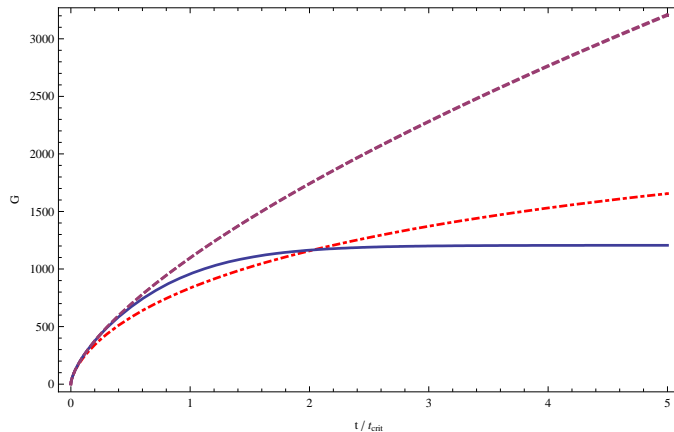


**Figure 11:** The linear growth factor for three different universes: a flat  $\rho_\Lambda \neq 0$  universe (solid), a curved  $\rho_\Lambda = 0$  universe (dot-dashed), and a flat,  $\rho_\Lambda = 0$  (unsuppressed) universe (dashed). The former two universes have been chosen so that  $t_c = t_\Lambda \equiv t_{\text{crit}}$ , and the time axis is given in units of  $t_{\text{crit}}$ . In the  $\rho_\Lambda$  case, the growth factor can be well-approximated as being equal to the unsuppressed case up until  $t = t_{\text{crit}}$ , and then abruptly becoming flat. This approximation is manifestly worse for the curvature case. In the curvature case, the growth factor starts to deviate from the unsuppressed case well before  $t = t_c$ , and continues to grow well after  $t = t_c$ . This effect makes the case of strong curvature harder to approximate analytically.

formation rate as a function of  $\Delta N$  and  $Q$  for fixed  $\rho_\Lambda = \rho_{\Lambda_0}$ . The dashed line in Fig. 10(b) marks the boundary  $t_c = t_{\text{peak}}$ , where the time of curvature domination equals the time of the unsuppressed peak (again computed according to Eq. 3.1). In this case the line is given by  $(2\Delta N + 7) \log_{10} e = -\log_{10} Q/Q_0$ , owing to the fact that  $t_c \propto \exp(3\Delta N)$ . Unlike the case of  $\rho_\Lambda$ , this line obviously does not mark the transition from structure formation to no structure formation. The reason has to do with the details of the nature of the suppression coming from curvature versus that coming from the cosmological constant. In the case of the cosmological constant, it is a very good approximation to say that structure formation proceeds as if there were no cosmological constant up until  $t = t_\Lambda$ , whereupon it stops suddenly. Curvature is far more gradual: its effects begin well before  $t_c$  and structure formation continues well after  $t_c$ . Fig. 11 illustrates this point clearly. There we see that while perturbations are suppressed in both the high curvature and large  $\rho_\Lambda$  cases, it is only in the  $\rho_\Lambda$  case that the naive approximation of a “sudden end” to structure formation is valid. For the curvature case there is no simple approximation, and the full model is necessary to give an accurate assessment of the situation.

## Acknowledgments

We thank K. Nagamine for providing us with a compilation of data points for the observed star formation rate. We are grateful to C. McKee, J. Niemeyer, and E. Quataert for discussions. We also thank J. Carlson for collaboration at the early stages of this project. This work was supported by the Berkeley Center for Theoretical Physics, by a CAREER grant (award number 0349351) of the National Science Foundation, by FQXi grant RFP2-08-06, and by the U.S. Department of Energy under Contract DE-AC02-05CH11231.

## References

- [1] R. Bousso and J. Polchinski, *Quantization of four-form fluxes and dynamical neutralization of the cosmological constant*, *JHEP* **06** (2000) 006 [[hep-th/0004134](#)].
- [2] R. Bousso, *Holographic probabilities in eternal inflation*, *Phys. Rev. Lett.* **97** (2006) 191302 [[hep-th/0605263](#)].
- [3] R. Bousso, R. Harnik, G. D. Kribs and G. Perez, *Predicting the Cosmological Constant from the Causal Entropic Principle*, *Phys. Rev.* **D76** (2007) 043513 [[hep-th/0702115](#)].
- [4] L. Hernquist and V. Springel, *An analytical model for the history of cosmic star formation*, *Mon. Not. Roy. Astron. Soc.* **341** (2003) 1253 [[astro-ph/0209183](#)].
- [5] J. M. Cline, A. R. Frey and G. Holder, *Predictions of the causal entropic principle for environmental conditions of the universe*, *Phys. Rev.* **D77** (2008) 063520 [[0709.4443](#)].
- [6] M. Tegmark, A. Aguirre, M. Rees and F. Wilczek, *Dimensionless constants, cosmology and other dark matters*, *Phys. Rev.* **D73** (2006) 023505 [[astro-ph/0511774](#)].
- [7] M. Tegmark and M. J. Rees, *Why is the CMB fluctuation level  $10^{-5}$ ?*, *Astrophys. J.* **499** (1998) 526–532 [[astro-ph/9709058](#)].
- [8] A. De Simone, A. H. Guth, M. P. Salem and A. Vilenkin, *Predicting the cosmological constant with the scale-factor cutoff measure*, [0805.2173](#).
- [9] S. R. Coleman and F. De Luccia, *Gravitational Effects on and of Vacuum Decay*, *Phys. Rev.* **D21** (1980) 3305.
- [10] **WMAP** Collaboration, E. Komatsu *et. al.*, *Five-Year Wilkinson Microwave Anisotropy Probe (WMAP) Observations: Cosmological Interpretation*, [0803.0547](#).
- [11] C. G. Lacey and S. Cole, *Merger rates in hierarchical models of galaxy formation*, *Mon. Not. Roy. Astron. Soc.* **262** (1993) 627–649.

- [12] R. S. Sutherland and M. A. Dopita, *Cooling functions for low - density astrophysical plasmas*, *Astrophys. J. Suppl.* **88** (1993) 253.
- [13] S. D. M. White, *Formation and evolution of galaxies: Lectures given at Les Houches, August 1993*, [astro-ph/9410043](#).
- [14] B. Freivogel, *Anthropic Explanation of the Dark Matter Abundance*, [0810.0703](#).
- [15] K. Nagamine, J. P. Ostriker, M. Fukugita and R. Cen, *The History of Cosmological Star Formation: Three Independent Approaches and a Critical Test Using the Extragalactic Background Light*, *Astrophys. J.* **653** (2006) 881–893 [[astro-ph/0603257](#)].
- [16] A. M. Hopkins and J. F. Beacom, *On the normalisation of the cosmic star formation history*, *Astrophys. J.* **651** (2006) 142 [[astro-ph/0601463](#)].
- [17] B. Freivogel, M. Kleban, M. Rodriguez Martinez and L. Susskind, *Observational consequences of a landscape*, *JHEP* **03** (2006) 039 [[hep-th/0505232](#)].
- [18] R. Bousso and S. Leichenauer. To appear.